Dalton Transactions

Accepted Manuscript

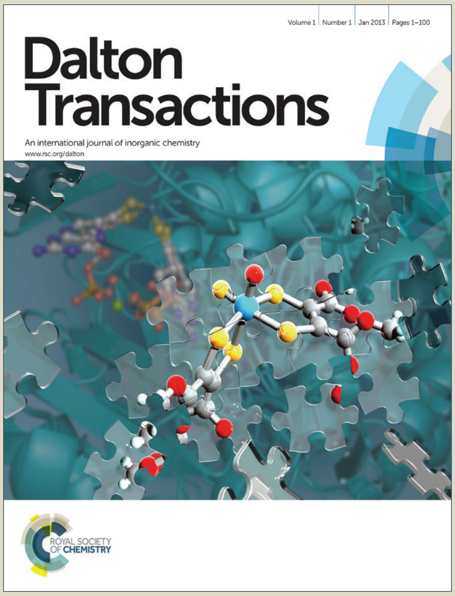

ROYAL SOCIETY OF CHEMISTRY

www.rsc.org/dalton

Dalton Transactions RSCPublishing

ARTICLE

Cite this: DOI: 10.1039/x0xx00000x

Received 00th January 2012,
Accepted 00th January 2012

DOI: 10.1039/x0xx00000x

www.rsc.org/

Syntheses, Structures, and Magnetic Properties of Three New Cyano-Bridged Complexes Based on the $[Mn(CN)_6]^{3-}$ Building Block

Shao-Liang Zhang, Xin-Hua Zhao and Xin-Yi Wang*

With three pentadentate macrocyclic ligands, three new $[Mn(CN)_6]^{3-}$ based complexes, $[Mn(L_{N3O2})(H_2O)]_2[Mn(CN)_6](ClO_4)\cdot 3H_2O$ (**1**), $\{[Mn(L_{N5})]_3[Mn(CN)_6]_2\}_n$ (**2**) and $\{[Mn(L_{N5Me})]_3[Mn(CN)_6]_2\}_n\cdot 10nH_2O$ (**3**) (L_{N3O2} = 2,13-dimethyl-6,9-dioxa-3,12,18-triazabicyclo[12.3.1]octadeca-1(18),2,12,14,16-pentaene, L_{N5} = 2,13-dimethyl-3,6,9,12,18-pentaazabicyclo-[12.3.1]octadeca-1(18),2,12,14,16-pentaene, L_{N5Me} = 2,6-bis[1-(2-(N-methylamino)ethylimino)ethyl]-pyridine), have been synthesized and characterized structurally and magnetically. The structure of **1** was found to be a linear $Mn^{II}_2Mn^{III}$ trinuclear cluster with two Mn^{II} capping groups and one Mn^{III} ion connected via two *trans*-cyano groups. In contrast, compounds **2** and **3** are cyano-bridged 2D networks. Magnetic investigation reveals the antiferromagnetic coupling between Mn^{III} and Mn^{II} ions through the bridging cyanide groups. Complex **1** shows paramagnetic behavior down to 2.0 K with no sign of SMM behavior. The magnetic coupling constant of $J = -1.63\ cm^{-1}$ with the Hamiltonian $H = -2J(S_{Mn(III)}\cdot S_{Mn(II)1} + S_{Mn(III)}\cdot S_{Mn(II)2})$ was obtained from the fitting of the magnetic susceptibility. For **2** and **3**, ferrimagnetic ordering was observed, with magnetic phase transition temperatures (T_c) being 7.5 K and 7.0 K, respectively. These compounds are the rare examples of a small number of the $[Mn(CN)_6]^{3-}$ based magnetic materials.

Introduction

Molecule-based magnetic materials have been explored intensively not only because of their fundamental interest but also due to their potential applications as functional materials.[1] Of all the molecular magnetic materials, the cyano-bridged compounds are of great importance. Various cyano-bridged materials of interesting magnetic properties, including single-molecule magnets (SMMs),[2] single-chain magnets (SCMs),[3] high T_c magnets,[4] photo-responsive magnets,[5] chiral magnets[6], spin-crossover (SCO) compounds[7] and so on, have been prepared and reported. For the synthesis of these materials, building block approach utilizing the carefully designed precursors as the starting materials is most widely used. In this sense, cyanometallate precursors offer a number of distinct advantages.[2b, 8] Except for some rare cases, they are generally stable in solution; the spin states of the cyanometallate precursors can be controlled by choosing the appropriate metal centers with suitable chemical valence; the nature of magnetic coupling (ferromagnetic vs. antiferromagnetic) is typically predictable using the simple and straightforward *Goodenough-Kanamori rule*;[9] and the structure and dimensionality can be largely controlled by introducing specific capping ligands on one or more of the starting materials. For all the studied cyanometallates, $[M(CN)_n]^{m-}$ and $[ML(CN)_n]^{m-}$ (L = ligands), the $[M(CN)_6]^{3-}$ (M = Fe^{III}, Cr^{III}, Mn^{III}, etc.) motifs are with no doubt the most intensively investigated. Based on these starting materials, the resulting Prussian Blue (PB) analogues, $A_xM^{II}_y[M'^{III}(CN)_6]\cdot nH_2O$ (A = alkali metal; M and M'= divalent and trivalent transition metal ions, respectively), are the reservoir of many intriguing physical properties mentioned above, such as the room temperature magnets, photomagnets, SCO and so on.[4, 5a, 7a, 10] In this sense, the PB type compounds are like the chameleon in the molecule magnetism, as the perovskite compounds in the inorganic materials.

Due to the magnetic anisotropy of the low spin Mn^{III} center (ground strong field configuration: t_{2g}^4, ground strong field term in O_h symmetry: ${}^3T_{1g}$), the effective magnetic coupling through CN^-, and the possible anisotropic magnetic coupling, the building block $[Mn^{III}(CN)_6]^{3-}$ has been very attractive for designing magnetic materials.[11-15] However, compared to the widely studied $[Cr^{III}(CN)_6]^{3-}$ and $[Fe^{III}(CN)_6]^{3-}$ units, the limited stability of $[Mn^{III}(CN)_6]^{3-}$ in solution hinders the study of the $[Mn^{III}(CN)_6]^{3-}$-based materials.[16] Generally, single crystals of the $[Mn^{III}(CN)_6]^{3-}$-containing materials are quite difficult to obtain as $[Mn(CN)_6]^{3-}$ decomposes in solution.[16] Up to now there are only limited examples reported in the literature, including a trigonal bipyramidal SMM $\{[Mn^{II}(tmphen)_2]_3[Mn^{III}(CN)_6]_2\}$,[11a] a triplesalen-based SMM $[\{(talen^{tBu2})(Mn^{III}(MeOH))_3\}_2\{Mn^{III}(CN)_6\}](lac)_3 \cdot 10.5MeOH$,[11b-c] a 1D SCM $[Mn^{III}(5\text{-}TMAMsalen)Mn^{III}(CN)_6]_n \cdot 4nH_2O$,[12a] the 2D chiral ferrimagnets $[Mn^{II}(HL)(H_2O)][Mn^{III}(CN)_6] \cdot 2H_2O$ (L = *S*- or *R*-1,2-diaminopropane),[12b] an interpenetrated 3D ferrimagnet $\{[Mn(4dmap)_4]_3[Mn(CN)_6]_2\}_n \cdot 10nH_2O$,[12c] 3D magnet $[Ru_2(O_2CMe)_4]_3[Mn(CN)_6] \cdot 3.3MeCN$,[12d] several 3d-4f compounds based on the $[Mn^{III}(CN)_6]^{3-}$ unit,[13] and some PB analogues such as $Mn^{II}_3[Mn^{III}(CN)_6]_2 \cdot zH_2O$,[14a-c] $Cs^{I}Mn^{II}[Mn^{III}(CN)_6] \cdot 1/2H_2O$,[14b] $Cs^{I}Ni^{II}[Mn^{III}(CN)_6] \cdot H_2O$,[14d-e] $Ni^{II}_3[Mn^{III}(CN)_6]_2 \cdot 12H_2O$,[14d] $(NMe_4)Mn^{II}[Mn^{III}(CN)_6] \cdot 8H_2O$,[14e] and $M^{III}[Mn^{III}(CN)_6]$ (M^{III} = V, Cr, Mn).[14f] Thus, more examples of the $[Mn^{III}(CN)_6]^{3-}$ based materials are certainly needed and of great value to this area. As a matter of fact, the paramagnetic cyanometallates of the $[Mn(L)(CN)_x]^{n-}$ type also remain scarce in the literature. The reported examples include the following: $Mn^{II}(bpy)_2(CN)_2 \cdot 3H_2O$ and $Mn^{II}(phen)_2(CN)_2 \cdot 3H_2O$,[17a] $(TPP)[Mn^{III}(Pc)(CN)_2] \cdot DCM$,[17b] *trans*-$[Mn(cyclam)(CN)_2](ClO_4)$,[17c] $(NEt_4)[(Tp^*)Mn^{II}(acac)(CN)]$,[17d] $(NEt_4)[(Tp^*)Mn^{III}(CN)_3]$,[17d] and $(PPN)[(Tp^*)Mn^{III}(CN)_3]$[17d] (bpy = 2,2-bipyridine, phen = 1,10-phenanthroline, Pc = phthalocyaninato, TPP^+ = tetraphenylphosphonium, DCM = dichloromethane, cyclam = 1,4,8,11-tetraazacyclotetradecane, acac = acetylacetonate, Tp* = hydridotris(3,5-dimethylpyrazol-1-yl)borate, PPN = bis(triphenylphosphine)-iminium).

It is well known that a well-designed blocking ligand plays a very important role in the preparation of the cyano-based molecular magnetic materials as it can greatly influence the nuclearity, topology, and the dimensionality of the resulting products. In this regard, the macrocyclic ligands are very useful as they can efficiently block the metal's available coordination sites and decrease the possibility to precipitate the 3D structures such as the PB analogs.[18-20] Using the macrocyclic ligands, cyano-bridged compounds based on the $[Fe(CN)_6]^{3-}$ and $[Cr(CN)_6]^{3-}$ units can be obtained, with structures including 0D clusters such as the trinuclear clusters,[18a-b, 19a] pentanuclear complex,[18c-d] 1D chains,[19a] 2D coordination polymers,[19a-b] and 3D networks.[19c] In our previous work, the macrocyclic ligands were also used to prepare the low dimensional magnetic materials involving the $[Mo(CN)_7]^{4-}$ building block. A docosanuclear Mo_8Mn_{14} cluster with a very high ground state spin value[20] and several trinuclear Mn_2Mo compounds including a first $[Mo(CN)_7]^{4-}$ based SMM were successfully prepared with the help of the macrocyclic ligands.[2d]

Inspired by the aforementioned consideration, we aimed at the magnetic materials based on the $[Mn(CN)_6]^{3-}$ unit and other building blocks with the macrocyclic ligands. By carefully tuning the reaction conditions and modification of the precursors, we obtained three new $[Mn^{III}(CN)_6]^{3-}$ based complexes: $[Mn(L_{N3O2})(H_2O)]_2[Mn(CN)_6](ClO_4) \cdot 3H_2O$ (**1**), $\{[Mn(L_{N5})]_3[Mn(CN)_6]_2\}_n$ (**2**) and $\{[Mn(L_{N5Me})]_3[Mn(CN)_6]_2\}_n \cdot 10nH_2O$ (**3**) (L_{N3O2} = 2,13-dimethyl-6,9-dioxa-3,12,18-triazabicyclo[12.3.1]octadeca-1(18),2,12,14,16-pentaene, L_{N5} = 2,13-dimethyl-3,6,9,12,18-pentaazabicyclo-[12.3.1]octadeca-1(18),2,12,14,16-pentaene, L_{N5Me} = 2,6-bis[1-(2-(N-methylamino)ethylimino)ethyl]-pyridine, Scheme 1). Compound **1** is a trinuclear cluster and **2** and **3** are two-dimensional structures. Their syntheses, structures, and magnetic properties were reported here.

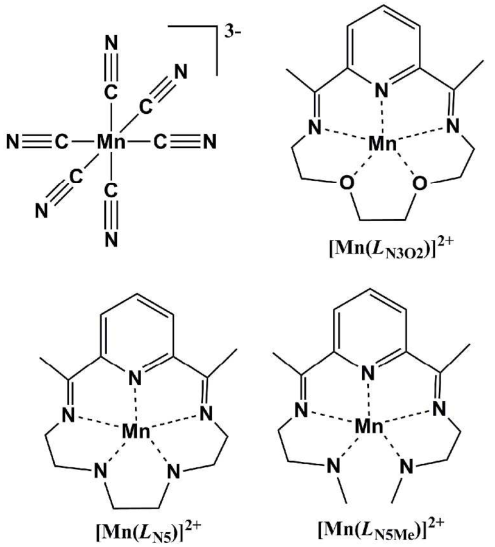

Scheme 1. Building blocks and precursors used to prepare complexes **1-3**.

Experimental Section

Physical Measurements

Elemental analyses of carbon, hydrogen, and nitrogen were carried out on a Vario EL II Elementar. Infrared spectra of the samples were obtained on a Bruker Tensor 27 FT-IR spectrometer with the KBr pellets. Powder X-ray diffraction (PXRD) were recorded at 298 K on a Bruker D8 Advance diffractometer with Cu Kα X-ray source (operated at 40 kV and 40 mA). Magnetic properties of **1** to **3** were measured using a Quantum Design SQUID VSM magnetometer on polycrystalline samples. All magnetic data were corrected for the diamagnetism of the sample holder and of the constituent atoms according to Pascal's constants.

Materials

The starting materials $K_3[Mn(CN)_6]$,[21] $Mn(L_{N3O2})Cl_2$,[19a] $[Mn(L_{N5})(H_2O)Cl]ClO_4$,[22] $Mn(L_{N5Me})Cl_2$[23] were synthesized according to the literature methods. The syntheses of **1-3** were carried out in the deoxygenated solvents under cold condition in the dark to avoid possible oxidation of the Mn^{2+} starting materials and decomposition of $K_3[Mn(CN)_6]$.

CAUTION!

Cyanides are highly toxic and perchlorate salts of metal complexes are potentially explosive. They should be handled in small quantities with care.

Preparations

$[Mn(L_{N3O2})(H_2O)]_2[Mn(CN)_6](ClO_4)\cdot 3H_2O$ (1). A mixture of $K_3Mn(CN)_6$ (16.4 mg, 0.05 mmol) and $LiClO_4$ (53 mg, 0.5 mmol) was dissolved in 2 mL of water, and then mixed with the solution of $Mn(L_{N3O2})Cl_2$ (40 mg, 0.10 mmol in 2 mL of H_2O/DMF with V/V = 1:1). The resulting solution was stirred for 5 minutes, and then filtered and left to stand in the dark at 4 ^oC without disturbing. Red-brown single crystals suitable for X-ray diffraction were obtained after several days. Yield: 28.7 mg, 54%. Elemental analysis (%) calculated for $C_{36}H_{52}N_{12}O_{13}ClMn_3$: C, 40.75; H, 4.94; N, 15.84. Found: C, 40.76; H, 4.92; N, 15.95. IR (KBr): 2113(s) cm^{-1} for ν(C≡N).

$\{[Mn(L_{N5})]_3[Mn(CN)_6]_2\}_n$ (2). A solution of $[(18\text{-crown-}6)K]_3[Mn(CN)_6]$ was prepared by stirring $K_3[Mn(CN)_6]$ (16.4 mg, 0.05 mmol) and 18-crown-6 (39.6 mg, 0.15 mmol) in 3 mL methanol for 3 h. An H-shaped tube was charged with a 3 mL of solution of $[(18\text{-crown-}6)K]_3[Mn(CN)_6]$ in one side and 3 mL of DMF solution of $[Mn(L_{N5})(H_2O)Cl]ClO_4$ (36 mg, 0.075 mmol) in the other side. Another 4 mL solvent (V_{MeOH}/V_{MeCN} = 1:1) was carefully layered on the top of the solutions as a buffer. The tube was then sealed and stored in the dark at 4 ^oC. Red-brown single crystals suitable for X-ray diffraction formed in the tube over the period of three weeks. The crystals were removed from the H-tube and washed with methanol. Yield: 12.6 mg, 36%. Elemental analysis (%) calculated for $C_{57}H_{69}N_{27}Mn_5$: C, 48.66; H, 4.94; N, 26.88. Found: C, 48.78; H, 4.71; N, 27.02. IR (KBr): 2111(s) cm^{-1} for ν(C≡N).

$\{[Mn(L_{N5Me})]_3[Mn(CN)_6]_2\}_n\cdot 10nH_2O$ (3). Compound **3** was prepared by a similar method as that for **2** except for the solvent. An H-tube was charged with a 3 mL methanol solution of $[(18\text{-crown-}6)K]_3[Mn(CN)_6]$ in one side and 3 mL solution of $Mn(L_{N5Me})Cl_2$ (30 mg, 0.075 mmol in MeOH/H_2O with V/V = 1:1) in the other side. Another 4 mL solvent (V_{MeOH}/V_{MeCN} = 1:1) was carefully layered on the top of the solutions as a buffer. The tube was then sealed and stored in the dark at 4 ^oC. Red-brown single crystals suitable for X-ray diffraction formed in the tube over the period of three weeks. The crystals were removed from the H-tube and washed with methanol. Yield: 11.9 mg, 30%. Elemental analysis (%) calculated for $C_{57}H_{95}N_{27}O_{10}Mn_5$: C, 42.97; H, 6.01; N, 23.74. Found: C, 42.89; H, 5.80; N, 23.95. IR (KBr): 2114(s) cm^{-1} for ν(C≡N).

X-ray Data Collection and Structure Determination

X-ray data for compounds **1-3** were collected on a Bruker APEX Duo diffractometer with a CCD area detector (Mo-Kα radiation, λ = 0.71073 Å) under nitrogen at 120 K. The APEXII program was used to determine the unit cell parameters and for data collection. Data were integrated using SAINT[24] and SADABS.[25] The structures of all three compounds were solved by direct methods and refined by full matrix least-square methods based on F^2 using the SHELXTL program.[26] Anisotropic thermal parameters were used for the non-hydrogen atoms and isotropic parameters for the hydrogen atoms. Hydrogen atoms of the organic ligands were refined as riding on the corresponding non-hydrogen atoms. Crystal data and experimental details of the structure determinations are listed in Table 1. Selected bond lengths and bond angles for complexes **1-3** are given in Tables S1-S3 (Supporting Information). The phase purity of all three compounds was confirmed by their PXRD spectra (Figure S1-S3).

Table 1. Crystallographic data and structure refinement parameters for complexes **1-3**.

Complex	**1**	**2**	**3**
Formula	$C_{36}H_{52}N_{12}O_{13}ClMn_3$	$C_{57}H_{69}N_{27}Mn_5$	$C_{57}H_{95}N_{27}O_{10}Mn_5$
M	1061.17	1407.09	1593.23
Crystal system	monoclinic	triclinic	triclinic
Space group	$C2/c$	$P\bar{1}$	$P\bar{1}$
a [Å]	39.847(3)	11.418(2)	11.467(6)
b [Å]	13.2542(11)	16.938(3)	17.402(10)
c [Å]	18.3527(14)	20.679(4)	20.493(11)
α [°]	90	97.553(3)	100.383(8)
β [°]	102.5730(10)	94.078(3)	90.651(8)
γ [°]	90	106.831(3)	108.525(8)
V [Å^3]	9460.3(13)	3769.6(12)	3804(4)
Z	8	2	2
ρ_{calcd}(g cm^{-3})	1.490	1.240	1.374
F(000)	4384	1450	1622
Crystal size (mm)	0.25×0.13×0.07	0.11×0.09×0.05	0.15×0.08×0.07
Reflections collected	31458	20902	21006
Independent reflections	10925	13218	13371
R_{int}	0.0436	0.0431	0.0783
GOF	1.037	1.052	1.048
R_1, wR_2 (I>2σ(I))	0.0398,0.1177	0.0885,0.2330	0.0842,0.1775

Results and Discussion

Syntheses and Crystal Structure Descriptions

The macrocyclic ligands reported in this work can be obtained easily by a metal templated Schiff-base condensation of 2,6-diacetylpyridine and polyamine. Due to their planar character, the resulting metal complexes are usually seven coordinated with approximate pentagonal bipyramid geometry, where the axial positions are usually coordinated by the weakly bonded ligands, such as the solvent molecules or the anions. These ligands can be easily substituted by the nitrogen atoms from the cyanide groups to form extended structures.[2d, 18-20] Due to the low stability of the $[Mn^{III}(CN)_6]^{3-}$ starting material in the solution, the reactions of these macrocyclic building blocks with the $[Mn^{III}(CN)_6]^{3-}$ have to be performed at low temperatures.

Complex **1** crystallizes in the monoclinic space group $C2/c$ and has a linear $Mn^{II}_2Mn^{III}$ trinuclear structure where two $[Mn(L_{N3O2})]^{2+}$ capping groups are connected to the Mn^{III} center via two CN^- groups in the trans position (Figure 1). The positive charge of the cluster is balanced by a ClO_4^- anion. Interestingly, there are two unique trinuclear units (units A and B) in the crystal structure. In unit A, the central Mn^{III} ion lies on a special position (0.00, 0.74, 0.25) with a C_2 axis. While in unit B, the Mn^{III} center is sited in the inversion center (0.25, 0.75, 0.50). All the Mn^{II} ions in **1** are in a slightly distorted pentagonal bipyramidal environment with seven coordinated atoms, five of which are from the macrocyclic ligand L_{N3O2}, with the remaining two being a nitrogen atom from a bridging cyanide and an oxygen atom from the coordinated water. The Mn-N and Mn-O distances lie in the range of 2.203 - 2.248 Å (av. 2.229 Å) and 2.257 - 2.288 Å (av. 2.277 Å). Using the program SHAPE 2.1,[27] the continuous shape measures (CShM's) of the Mn^{II} centers relative to the ideal pentagonal bipyramid are calculated to be 0.110, 0.322 for Mn2 and Mn4, respectively. As for the $[Mn(CN)_6]^{3-}$ unit, the Mn^{III} center is in an distorted octahedron environment with CShM's being 0.105, 0.019 relative to the ideal octahedron for Mn1 and Mn3, respectively. While the octahedron of the $[Mn(CN)_6]^{3-}$ is tetragonally compressed for unit A (the axial bond Mn1-C1 = 1.992(2) Å, the equatorial ones Mn1-C2 = 2.003(2) Å, Mn1-C3 = 2.008(2) Å), it is tetragonally elongated for unit B (the axial bond Mn3-C19 = 2.015(2) Å, the equatorial ones Mn3-C20 = 2.000(3) Å, Mn3-C21 = 2.004(2) Å). Bridged by the CN^- groups, the Mn^{II}-Mn^{III} distances for units A and B are 5.253 and 5.361 Å, respectively.

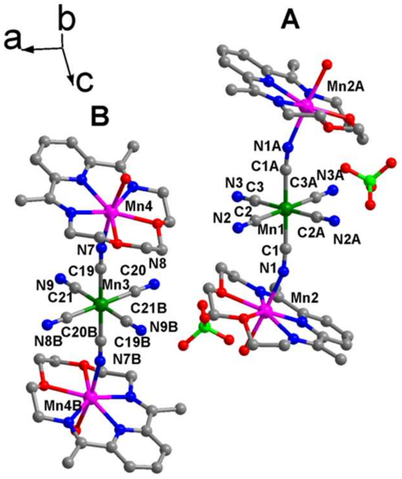

Figure 1. Perspective view of the linear trinuclear structure in complex **1**. Units A and B are two unique trinuclear clusters. All the hydrogen atoms and the solvent molecules have been omitted for clarity.

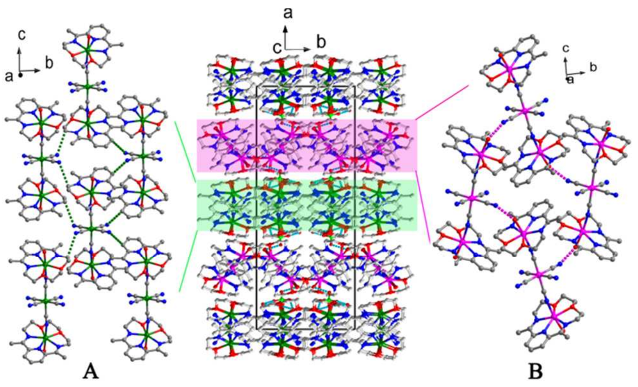

Figure 2. The 2D layers of **1** constructed from the trinuclear units A (left) and B (right). Middle: the 3D structure of **1** formed by the alternatively stacked layers along the *a* axis. The dashed lines represent the hydrogen bonds.

Connected by the C-H···N hydrogen bonds for units A between the C-H groups of the macrocyclic ligands and the CN^- groups (C15···N3 = 3.484 Å, C6···N2 = 3.403 Å) and the O-H···N hydrogen bonds for units B between the coordinated water molecules and the CN^- groups (O6···N9 = 2.829 Å), both units form 2D supermolecular networks along the *bc* plane (Figure 2). These layers are then stacked alternatively along the *a* axis and are linked together by a great number of O-H···O hydrogen bonds involving the ClO_4^- anions and the H_2O molecules with the O···O distances being in the range of 2.733 to 3.213 Å.

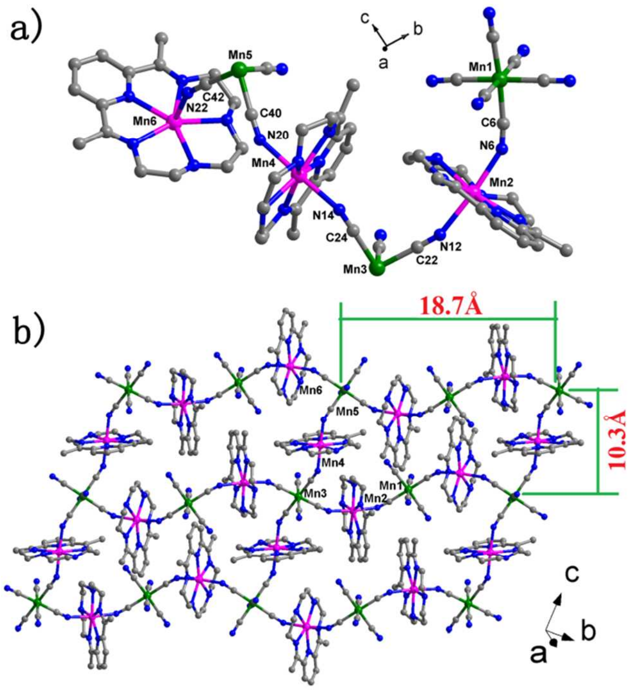

Figure 3. The asymmetry unit (a) and 2D (4,4) network (b) of complex **2**. The numbers in (b) represent the distances between these two vertexes. All the hydrogen atoms have been omitted for clarity.

Although the macrocyclic ligands L_{N5} and L_{N5Me} are very similar to the L_{N3O2} ligand in **1**, the crystal structures of complexes **2** and **3** are totally different from that of **1**, indicating a dramatic influence of the macrocyclic ligands on the resulting products. Bridged by the $[Mn(CN)_6]^{3-}$ units, both compounds **2** and **3** have a very similar 2D layered structure, despite of the significantly different number of the crystalized water molecules in the structure. We will only discuss the structure of **2**. Synthesized from the anhydrous solvent, **2** crystallizes in a triclinic space group $P\bar{1}$ and has no solvent molecules in the structure. As can be seen from Figure 3, the asymmetric unit of **2** consists of three $[Mn^{II}(L_{N5})]^{2+}$ units, one $[Mn^{III}(CN)_6]^{3-}$ unit (Mn1) in a general position, two half of the $[Mn^{III}(CN)_6]^{3-}$ units (Mn3 and Mn5) in the (1, 0, 0) and (1, 0, 0.5) positions. All the Mn^{II} ions are in the slightly distorted pentagonal bipyramidal geometry (the CShM's are 0.541, 0.304, and 0.358 for Mn2, Mn4 and Mn6, respectively), surrounded by five equatorial N atoms from L_{N5}, and two axial N atoms from cyanides. Although there exist three crystallographic unique $[Mn(CN)_6]^{3-}$ units, they only show two different coordination modes, namely the $[Mn^{III}(\mu\text{-CN})_2(CN)_4]^{3-}$ for Mn1 and $[Mn^{III}(\mu\text{-CN})_4(CN)_2]^{3-}$ for Mn3 and Mn5 centres. Thus, Mn1 bridges two Mn^{II} units using the two CN^- groups in the *trans*-position, while Mn3 and Mn5 link four Mn^{II} neighbours with the four equatorial CN^- groups. Linked by these two- and four-connected nodes, compound **2** has a neutral 2D layer along the (1, ī, 0) plane (Figure 3). Although the shortest Mn^{III}-Mn^{II} distance bridged by the CN^- groups is only about 5.2 Å, the repeating unit in the layer is a twelve-membered cyclic unit $[Mn1\text{-}CN\text{-}Mn2\text{-}NC\text{-}Mn3\text{-}CN\text{-}Mn4\text{-}NC\text{-}Mn5\text{-}CN\text{-}Mn6\text{-}NC]_2$ with the size of about 10.3 × 18.7 Å. Similar 2D layer structures have been reported for $[Fe(CN)_6]^{3-}/[Cr(CN)_6]^{3-}$ and $Ni(L)^{2+}$ macrocyclic ligands (*L* = 2,12-dimethyl-3,7,11,17-tetraazabicyclo[11.3.1]heptadeca-1(17),13,15-triene).[19b] These layers are further connected to each other by the weak C-H···N hydrogen bonds with the shortest interlayer Mn···Mn distance of 7.98 Å (Figure S4). As for **3**, the structure is very similar to that of **2** except for the numerous hydrogen bonds involving the crystalized water molecules (Figures S5-S6).

Magnetic Properties

The temperature dependent magnetic susceptibility data for **1** measured over the temperature range of 2 − 300 K under 1000 Oe were displayed in Figure 4 as the $\chi_M T(T)$ and $\chi_M^{-1}(T)$ curves per $Mn^{II}{}_2Mn^{III}$ unit. The room-temperature value of $\chi_M T$ is 9.59 $cm^3mol^{-1}K$, slightly lower than the spin-only value of 9.75 $cm^3mol^{-1}K$ for two high-spin Mn^{II} ($S = 5/2$) and one low-spin Mn^{III} ($S = 1$) centers. On decreasing temperature, the $\chi_M T$ value decreases down to 8.01 $cm^3mol^{-1}K$ at 14 K, increases again to a maximum of 9.71 $cm^3mol^{-1}K$ at 2 K. The magnetic susceptibility above 100 K obeys the Curie−Weiss law with a Weiss constant $\theta = -6.31$ K and a Curie constant $C = 9.81$ $cm^3mol^{-1}K$. The negative Weiss constant and the decrease of the $\chi_M T$ curve at high temperature indicate the antiferromagnetic coupling between the Mn^{II} and Mn^{III} centers through the CN^- groups. The increase of the $\chi_M T$ curve below 14 K indicates the high-spin ground state of compound **1**. The $\chi_M T$ value at 2 K is only slightly smaller than the value of 10 $cm^3mol^{-1}K$ for a state of $S = 4$ ($g = 2.0$), resulting from the antiparallel alignment of two Mn^{II} and one Mn^{III} centers. As the two trinuclear units in the structure are similar, the magnetic coupling between the Mn^{II} and Mn^{III} centers can be described by one single coupling constant J with the Hamiltonian $H = -2J(S_{Mn(III)}S_{Mn(II)1} + S_{Mn(III)}S_{Mn(II)2})$. Using the program PHI,[27] the $\chi_M T$ data from 2 to 300 K can be fitted with the best-fit parameters $J = -1.63$ cm^{-1}, $g_{Mn(II)} = 2.003$, $g_{Mn(III)} = 1.967$ and $R = 0.010$. The negative J value is consistent with those found in the reported cyanide-bridged Mn^{II}–Mn^{III} complexes.[11-12]

The field dependent magnetization of **1** was also measured at 2.0 K with field up to 70 kOe (Figure S7). Typical paramagnetic behaviour was observed. At the highest magnetic field, M reaches the value of 8.98 μ_B, which is larger than the expected value of 8 μ_B for the antiferromagnetically coupled trinuclear $Mn^{II}{}_2Mn^{III}$ cluster. The reduced magnetization of **1** was also measured at low temperature with dc field up to 70 kOe (Figure S8). As we can see, magnetic anisotropy was suggested by the non-superposition of the reduced magnetization data to a single master curve. However, all attempts to fit the reduced magnetization data using both programs PHI and Anisofit2.0 failed. This could be due to the fact that the ground state of **1** is not a well-isolated state of $S = 4$ because of the weak magnetic interaction. In addition, the situation could become more complicated because of the existence of two different trinuclear clusters in **1**. To check whether **1** behaves as a SMM, ac susceptibility data under zero dc field were measured at low temperature. As can be seen from Figure S9, there is no observable out-of-phase signals down to 2.0 K, ruling out the SMM behaviour for **1**.

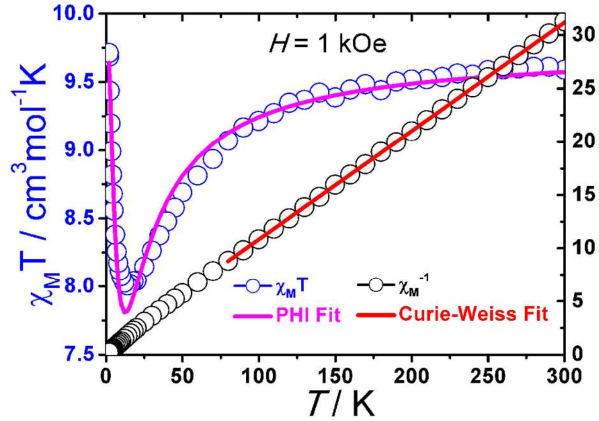

Figure 4. Temperature dependent magnetic susceptibility of **1** measured at 1 kOe. The red line represents Curie-Weiss fit and the magenta line represents the fitting using PHI.

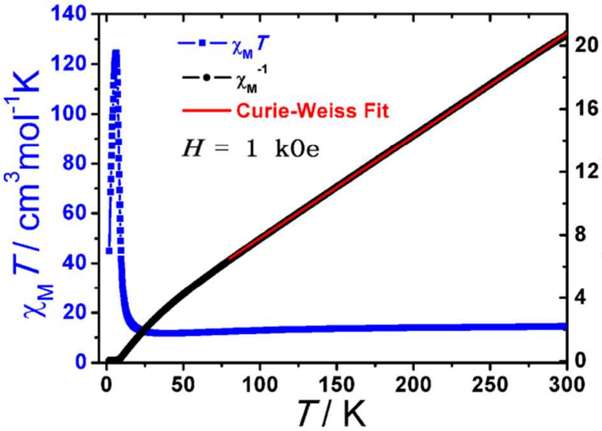

Figure 5. Temperature dependent magnetic susceptibility of **2** measured at 1 kOe. The red line represents Curie-Weiss fit.

As the magnetic properties of **2** and **3** are very similar due to their similar structures, the magnetic property of **2** will be discussed as representative, whereas the results of **3** can be found in the Supporting Information (Figures S10-S13). The magnetic susceptibility data measured under 1000 Oe for **2** were displayed in Figure 5 as the $\chi_M T(T)$ and $\chi_M^{-1}(T)$ curves. At room temperature, the $\chi_M T$ value per $Mn^{III}{}_2Mn^{II}{}_3$ unit is 14.45 $cm^3mol^{-1}K$, which is consistent with the spin-only value of 15.13 $cm^3mol^{-1}K$ expected for the magnetically isolated three

Mn^{II} (S = 5/2) and two Mn^{III} (S = 1) ions. Upon cooling from 300 K, the $\chi_M T$ curve gradually decreases down to the minimum value of 11.68 $cm^3mol^{-1}K$ at 37 K, and then rapidly increases up to the maximum peak of 124.6 $cm^3mol^{-1}K$ at 6.3 K, followed by a drop down to 44.9 $cm^3mol^{-1}K$ at 2 K. This behaviour is very typical for a long-range ordered ferrimagnet. The drop of $\chi_M T$ curve below 6 K should be due to the field saturation effect of the magnetization. A Curie–Weiss fit above 100 K gave a negative Weiss constant of θ = –19.9 K, which reflects the dominant antiferromagnetic interaction between the Mn^{II} and Mn^{III} ions, although it might partly come from spin-orbital coupling of the low-spin Mn^{III} ions.

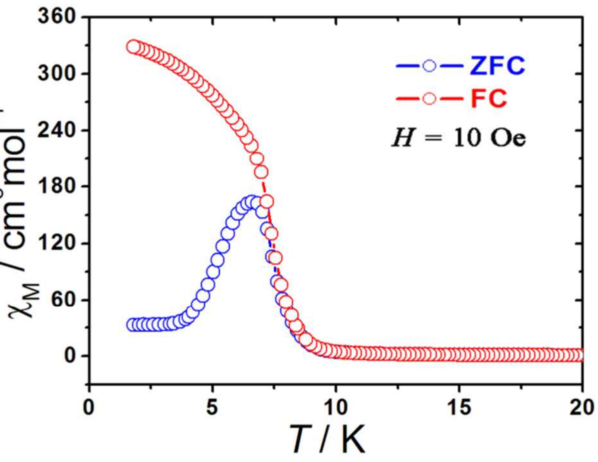

Figure 6. Zero-Field-Cooled and field-cooled (ZFC/FC) curves for compound **2** under a dc field of 10 Oe.

The occurrence of the long-range magnetic ordering at low temperature was further confirmed by the measurements at low temperatures, including the zero-field-cooled and field-cooled (ZFC/FC) magnetization measured in a dc field of 10 Oe and the ac susceptibilities measured under H_{dc} = 0 Oe and H_{ac} = 2 Oe. As can be seen from Figure 6, the ZFC curve exhibits a peak and diverges from the FC curve at about 7.5 K, suggesting the magnetic phase transition from the paramagnetic phase to a long-range ordered phase and the hysteretic effect at low temperature. As for the ac susceptibilities, the in-phase signals (χ_M') show a peak and the out-of phase signals (χ_M") rapidly increase below 7.5 K (Figure 7). These results are consistent to each other and confirm the magnetic ordering temperature T_c = 7.5 K. In addition, a very small frequency dependence for both the χ_M' and the χ_M" data was observed. The shift parameter $\varphi = (\Delta T_p/T_p)/\Delta(\log f)$ is only 0.007 (where T_p represents the peak temperature of the in-phase χ_M' plots and f is the frequency of the ac field), which is close to a value for a spin glass.[29] Because there are no disordered components and competitive interactions in the structure, the glassy behavior might come from the movement of the domain walls and/or the natural defects in the structure.[29]

To check the irreversibility of the magnetization suggested by the divergence of the ZFC/FC curves, the isothermal magnetization M was also measured at 2 K. At low fields, M increases very rapidly and then increases steadily with H > 10 kOe to reach a maximum value of 10.1 μ_B at 70 kOe (Figure 8), which is slightly lower than the calculated saturation value of 11 μ_B for the antiferromagnetically coupled three Mn^{II} and two Mn^{III} ions. Furthermore, an obvious hysteresis loop at 2 K can be observed with a remnant magnetization M_R = 4.68 μ_B and a coercive field H_c = 620 Oe (Figure 8). Compared with the corresponding $Mn^{II}_3Cr^{III}_2$,[12c] the coercive field and the remnant magnetization of **2** are significantly larger. This could be associated with the magnetic anisotropy of Mn^{III} ion, compared with the isotropic Cr^{III} center.

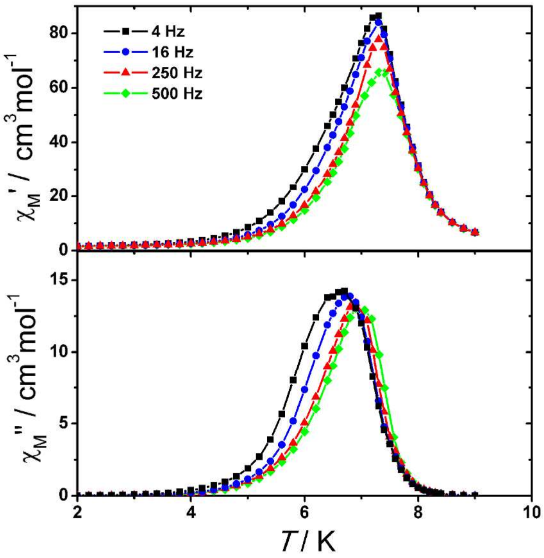

Figure 7. Temperature dependent ac susceptibilities of **2** at different frequencies under H_{ac} = 2 Oe and H_{dc} = 0 Oe.

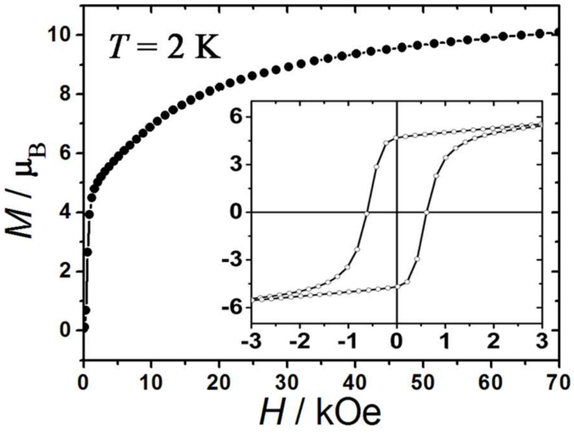

Figure 8. Field dependent magnetization and the hysteresis loop (inset) of **2** measured at 2 K.

As for complex **3**, its magnetic property is very similar to that of **2** with a slightly lower T_c value of 7.0 K. Considering their similar structures and magnetic properties, the slightly lower T_c of the hydrated **3** is consistent to the normal "magnetic sponges", whose magnetic ordering temperature T_c can change reversibly upon hydration/dehydration or upon sorption/desorption of guest molecules.[30] The T_c increases upon dehydration because of the closer distances between the spin centers and/or modified structures of the "dense" dehydrated form. For example, for a nanoporous magnet $\{[Mn(HL)]_2Mn[Mo(CN)_7]_2\}\cdot nH_2O$ (L = N,N'-Dimethylalaninol), the T_c value can be switched from 85 to 106 K by dehydration.[30b] In our case, compound **2** can be treated as a "dehydrated" form of **3** as it contains no lattice solvent molecules and is isostructural to **2**. Due to the large amount of the water molecules in the structure, the shortest interlayer Mn···Mn distance of **3** (8.40 Å) is actually larger than that of **2** (7.98 Å), which leads to the weaker interlayer magnetic coupling and justifies the slightly lower T_c of **3**.

As discussed for the Mn^{II}-Cr^{III} compounds,[12c] the T_c value of compounds **2** and **3** can be approximately given in the following equation according to the molecular field theory:

$$T_c = \frac{2\left(n_{Mn(III)}n_{Mn(II)}\right)^{1/2}|J|\left\{S_{Mn(III)}\left(S_{Mn(III)}+1\right)S_{Mn(II)}\left(S_{Mn(II)}+1\right)\right\}^{1/2}}{3k_B},$$

where $n_{Mn(III)}$ and $n_{Mn(II)}$ are the numbers of the nearest magnetic ions around Mn^{III} and Mn^{II} centers and J is the exchange interaction constant. According to this equation, we can see that the T_c value is proportional to the $n_{Mn(III)}$, $n_{Mn(II)}$ and $|J|$ values. Of course, we have to emphasize that the parameter $|J|$ should be considered as the averaged value along three directions. For those with lower dimensionality, the T_c is usually very low as the averaged $|J|$ is usually quite small due to the weak magnetic interactions between the clusters, chains or layers. In fact, for a perfect magnetic chain without any interchain magnetic interaction, the long-range ordering should only occur at 0 K. As we can see in Table 2, the PB analogues have the highest T_c as they are 3D structures with large ($n_{Mn(III)}$, $n_{Mn(II)}$) values. Also, because of the lower ($n_{Mn(III)}$, $n_{Mn(II)}$) values, **2** and **3** have the lower T_c values than compound $[Mn(HL)(H_2O)][Mn(CN)_6]\cdot H_2O$ (L = (-)-(S)- or (+)-(R)-1,2-diaminopropane) which is also a 2D layered structure but with a larger ($n_{Mn(III)}$, $n_{Mn(II)}$) value. In addition, for compound $\{[Mn(4dmap)_4]_3[Mn(CN)_6]_2\}_n\cdot 10nH_2O$, although it has a 3D structure, its T_c is quite low due to the very low ($n_{Mn(III)}$, $n_{Mn(II)}$) value and the very porous structure.

Table 2 T_c values of the $Mn^{II}Mn^{III}$ compounds based on the $[Mn(CN)_6]^{3-}$ unit.

Compound	($n_{Mn(III)}$, $n_{Mn(II)}$)	T_c/K	reference
$Mn^{II}_3[Mn^{III}(CN)_6]_2\cdot 12H_2O$	(6, 4)[a]	37	14b
$Mn^{II}_3[Mn^{III}(CN)_6]_2\cdot zH_2O$ (z = 12-16)	(6, 4)[a]	35.5	14a
$Mn^{II}_3[Mn^{III}(CN)_6]_2\cdot 12H_2O\cdot 1.7CH_3OH$	(6, 4)[a]	29	14c
$CsMn^{II}[Mn^{III}(CN)_6]\cdot 0.5H_2O$	(6, 6)	31	14b
$(Me_4N)Mn^{II}[Mn^{III}(CN)_6]\cdot 8H_2O$	(6, 6)	29	14e
$[Mn(HL)(H_2O)][Mn(CN)_6]\cdot H_2O$ (L = (-)-(S)- or (+)-(R)- 1,2-diaminopropane)	(4, 4)	21	12b
$\{[Mn(4dmap)_4]_2[Mn(CN)_6]_3\}_n\cdot 10nH_2O$	(3, 2)	6.4	12c
$\{[Mn(L_{N5})]_3[Mn(CN)_6]_2\}_n$	(3, 2)	7.5	this work
$\{[Mn(L_{N5Me})]_3[Mn(CN)_6]_2\}_n\cdot 10nH_2O$	(3, 2)	7.0	this work

[a] $n_{Mn(III)}/n_{Mn(II)}$ is an average value.

Conclusions

In conclusion, by carefully tuning the reaction condition and using the auxiliary macrocyclic ligands, we have synthesized and characterized three rare examples of $[Mn^{III}(CN)_6]^{3-}$ based molecular magnetic complexes, including a linear trinuclear cluster and two 2D layered compounds. Antiferromagnetic exchange interactions between the Mn^{II} and Mn^{III} ions were verified. Paramagnetic behavior was observed for the trinuclear compound, while the 2D layered compounds show ferrimagnetic long-range ordering with T_c around 7 K. Due to the very limited reports on the $[Mn^{III}(CN)_6]^{3-}$ based magnetic compounds, further efforts aiming at the preparation of more compounds with different macrocyclic ligands and different metal centers are of great value and are currently undertaken in the lab.

Acknowledgements

We thank the Major State Basic Research Development Program (2013CB922102), NSFC (91022031, 21101093, 21471077). This work was also supported by a Project Funded by the Priority Academic Program Development of Jiangsu Higher Education Institutions.

Notes and references

State Key Laboratory of Coordination Chemistry, Collaborative Innovation Center of Advanced Microstructures, School of Chemistry and Chemical Engineering, Nanjing University, Nanjing, 210093, China. Fax:+86-25-83314502. E-mail: wangxy66@nju.edu.cn

CCDC-1040571 (**1**), 1040572 (**2**) and 1040573 (**3**) contain the supplementary crystallographic data for this paper. These data can be obtained free of charge from the Cambridge Crystallographic Data Centre viawww.ccdc.cam.ac.uk/data_request/cif.

†Electronic Supplementary Information (ESI) available: Structure information in detail and additional magnetic data. For ESI and crystallographic data in CIFs or other electronic format see DOI: 10.1039/b000000x/.

1 (a) J. S. Miller and D. Gatteschi, eds., Themed issue on Molecule-based Magnets, *Chem. Soc. Rev.* 2011, **40**, 3053-3368; (b) E. Coronado and K. R. Dunbar, eds., Forum issue on Molecular Magnetism, *Inorg. Chem.* 2009, **48**, 3293-3896; (c) E. K. Brechin, ed., Themed issue on Molecular Magnetism, *Dalton Trans.* 2010, **39**, 4671-5038; (d) L. K. Thompson, ed., Special Issue on Magnetism-Molecular and Supramolecular Perspectives, *Coord. Chem. Rev.* 2005, **249**, 2549-2730.

2 (a) D. E. Freedman, D. M. Jenkins, A. T. Iavarone, J. R. Long, *J. Am. Chem. Soc.* 2008, **130**, 2884-2885; (b) X. Y. Wang, C. Avendano, K. R. Dunbar, *Chem. Soc. Rev.* 2011, **40**, 3213-3238 and references therein; (c) J. Dreiser, K. S. Pedersen, A. Schnegg, K. Holldack, J. Nehrkorn, M. Sigrist, P. Tregenna-Piggott, H. Mutka, H. Weihe, V. S. Mironov, J. Bendix, O. Waldmann, *Chem. Eur. J.* 2013, **19**, 3693-3701; (d) K. Qian, X. C. Huang, C. Zhou, X. Z. You, X. Y. Wang, K. R. Dunbar, *J. Am. Chem. Soc.* 2013, **135**, 13302-13305;

3 (a) M. Ferbinteanu, H. Miyasaka, W. Wernsdorfer, K. Nakata, K. I. Sugiura, M. Yamashita, C. Coulon, R. Clérac, *J. Am. Chem. Soc.* 2005, **127**, 3090-3099; (b) R. Lescouëzec, L. M. Toma, J. Vaissermann, M. Verdaguer, F. S. Dalgado, C. Ruiz-Pérez, F. Lloret,

M. Julve, *Coord. Chem. Rev.* 2005, **249**, 2691-2729; (c) L. M. Toma, R. Lescouezec, J. Pasan, C. Ruiz-Perez, J. Vaissermann, J. Cano, R. Carrasco, W. Wernsdorfer, F. Lloret, M. Julve, *J. Am. Chem. Soc.* 2006, **128**, 4842-4853; (d) T. D. Harris, M. V. Bennett, R. Clerac, J. R. Long, *J. Am. Chem. Soc.* 2010, **132**, 3980-3988; (e) X. Feng, J. Liu, T. D. Harris, S. Hill, J. R. Long, *J. Am. Chem. Soc.* 2012, **134**, 7521-7529.

4 (a) W. R. Entley, G. S. Girolami, *Science* 1995, **268**, 397-400; (b) O. Sato, T. lyoda, A. Fujishima, K. Hashimoto, *Science* 1996, **271**, 49-51; (c) S. Ferlay, T. Mallah, R. Ouahes, P. Veillet, M. Verdaguer, *Nature* 1995, **378**, 701-703.

5 (a) O. Sato, T. Iyoda, A. Fujishima, K. Hashimoto, *Science* 1996, **272**, 704-705; (b) O. Sato, J. Tao, Y. Z. Zhang, *Angew. Chem. Int. Ed.* 2007, **46**, 2152-2197; (c) S. I. Ohkoshi, H. Tokoro, *Acc. Chem. Res.* 2012, **45**, 1749-1758; (d) D. P. Dong, T. Liu, S. Kanegawa, S. Kang, O. Sato, C. He, C. Y. Duan, *Angew. Chem. Int. Ed.* 2012, **51**, 5119-5123; (e) N. Hoshino, F. Iijima, G. N. Newton, N. Yoshida, T. Shiga, H. Nojiri, A. Nakao, R. Kumai, Y. Murakami, H. Oshio, *Nat. Chem.* 2012, **4**, 921-926; (f) Y. Z. Zhang, P. Ferko, D. Siretanu, R. Ababei, N. P. Rath, M. J. Shaw, R. Clérac, C. Mathonière, S. M. Holmes, *J. Am. Chem. Soc.* 2014, **136**, 16854-16864 and references therein.

6 (a) Train, C.; Gruselle, M.; Verdaguer, M. *Chem. Soc. Rev.* 2011, **40**, 3297-3312; b) K. Inoue, K. Kikuchi, M. Ohba, H. Okawa, *Angew. Chem. Int. Ed.* 2003, **42**, 4810-4813; (c) M. X. Yao, Q. Zheng, X. M. Cai, Y. Z. Li, Y. Song, J. L. Zuo, *Inorg. Chem.* 2012, **51**, 2140-2149; (d) N. Hoshino, Y. Sekine, M. Nihei, H. Oshio, *Chem. Commun.* 2010, **46**, 6117-6119.

7 (a) W. Kosaka, K. Nomura, K. Hashimoto, S. I. Ohkoshi, *J. Am. Chem. Soc.* 2005, **127**, 8590-8591; (b) M. Shatruk, A. Dragulescu-Andrasi, K. E. Chambers, S. A. Stoian, E. L. Bominaar, C. Achim, K. R. Dunbar, *J. Am. Chem. Soc.* 2007, **129**, 6104-6116; (c) S. I. Ohkoshi, K. Imoto, Y. Tsunobuchi, S. Takano, H. Tokoro, *Nat. Chem.* 2011, **3**, 564-569; (d) M. C. Muňoz, J. A. Real, *Coord. Chem. Rev.* 2011, **255**, 2068; (e) T. Liu, H. Zheng, S. Kang, Y. Shiota, S. Hayami, M. Mito, O. Sato, K. Yoshizawa, S. Kanegawa, C. Y. Duan, *Nat. Commun.* 2013, **4**, 2826; and references therein.

8 M. Shatruk, C. Avendano, K. R. Dunbar, *Prog. Inorg. Chem.* 2009, **56**, 155-334.

9 a) J. B. Goodenough, *Magnetism and the Chemical Bond*, Interscience, New York, 1963; (b) J. Kanamori, *J. Phys. Chem. Solids* 1959, **10**, 87-98; (c) M. Raczkowski, R. Frésard, A. M. Oleś, *J. Phys.: Cond. Mater.* 2006, **18**, 7449-7469.

10 H. Tokoro, S. Ohkoshi, *Dalton Trans.* 2011, **40**, 6825-6833.

11 (a) C. P. Berlinguette, D. Vaughn, C. Canada-Vilalta, J. R. Galan-Mascaros, K. R. Dunbar, *Angew. Chem. Int. Ed.* 2003, **42**, 1523-1526; (b) V. Hoeke, K. Gieb, P. Müller, L. Ungur, L. F. Chibotaru, M. Heidemeier, E. Krickemeyer, A. Stammler, H. Bögge, C. Schröder, J. Schnack, T. Glaser, *Chem. Sci.* 2012, **3**, 2868-2882; (c) V. Hoeke, M. Heidemeier, E. Krickemeyer, A. Stammler, H. Bogge, J. Schnack, T. Glaser, *Dalton Trans.* 2012, **41**, 12942-12959.

12 (a) H. Miyasaka, T. Madanbashi, A. Saitoh, N. Motokawa, R. Ishikawa, M. Yamashita, S. Bahr, W. Wernsdorfer, R. Clerac, *Chem. Eur. J.* 2012, **18**, 3942-3954; (b) W. Kaneko, S. Kitagawa, M. Ohba, *J. Am. Chem. Soc.* 2007, **129**, 248-249; (c) W. Kaneko, M. Mito, S. Kitagawa, M. Ohba, *Chem. Eur. J.* 2008, **14**, 3481-3489; (d) T. E. Vos, Y. Liao, W. W. Shum, J. H. Her, P. W. Stephens, W. M. Reiff, J. S. Miller, *J. Am. Chem. Soc.* 2004, **126**, 11630-11639.

13 (a) B. Yan, Z. D. Chen, S. X. Wang, *Trans. Met. Chem.* 2001, **26**, 287-289; (b) B. Yan, S. X. Wang, Z. D. Chen, *J. Coord. Chem.* 2001, **54**, 53-61; (c) B. Yan, Z. D. Chen, S. X. Wang, S. Gao, *Chem. Lett.* 2001, 350-351.

14 (a) P. Franz, C. Ambrus, A. Hauser, D. Chernyshov, M. Hostettler, J. Hauser, L. Keller, K. Kramer, H. Stoeckli-Evans, P. Pattison, H. B. Burgi, S. Decurtins, *J. Am. Chem. Soc.* 2004, **126**, 16472-16477; (b) W. R. Entley, G. S. Girolami, *Inorg. Chem.* 1994, **33**, 5165-5166; (c) K. Awaga, T. Sekine, M. Okawa, W. Fujita, S. M. Holmes, G. S. Girolami, *Chem. Phys. Lett.* 1998, **293**, 352-356; (d) W. R. Entley, C. R. Treadway, G. S. Girolami, *Mol. Cryst. Liq. Cryst.* 1995, 273, 153-166; (e) D. Babel, *Comments Inorg. Chem.* 1986, **5**, 285-320; (f) W. E. Buschmann, J. S. Miller, *Inorg. Chem.* 2000, **39**, 2411-2421.

15 A. Palii, B. Tsukerblat, J. M. Clemente-Juan, E. *Inter. Rev. Phys. Chem.* 2010, **29**, 135-230.

16 A. Buckelew, J. R. Galan-Mascaros, K. R. Dunbar, *Adv. Mater.* 2002, **14**, 1646-1648.

17(a) J. A. Smith, J. R. Galán-Mascarós, R. Clérac, J. S. Sun, X. Ouyang, K. R. Dunbar, *Polyhedron* 2001, **20**, 1727-1734; (b) M. Matsuda, J. I. Yamaura, H. Tajima, T. Inabe, *Chem. Lett.* 2005, **34**, 1524-1525; (c) S. Mossin, H. O. Sørensen, H. Weihe, *Acta Cryst.* 2002, **C58**, m204-m206; d) M. Tang, D. Li, U. P. Mallik, Y. Z. Zhang, R. Clerac, G. T. Yee, M. H. Whangbo, A. Mungalimane, S. M. Holmes, *Inorg. Chem.* 2011, **50**, 5153-5164.

18 (a) Y. Z. Zhang, B. W. Wang, O. Sato, S. Gao, *Chem. Commun.* 2010, **46**, 6959-6961; (b) C. Paraschiv, M. Andruh, Y. Journaux, Z. Žak, N. Kyritsakas, L. Ricard, *J. Mater. Chem.* 2006, **16**, 2660-2668; (c) L. J. Batchelor, M. Sangalli, R. Guillot, N. Guihéry, R. Maurice, F. Tuna, T. Mallah, *Inorg. Chem.* 2011, **50**, 12045-12052; (d) S. Tanase, M. Andruh, N. Stanica, C. Mathonière, G. Rombaut, S. Golhen, L. Ouahab, *Polyhedron,* 2003, **22**, 1315-1320.

19 (a) F. Bonadio, M. C. Senna, J. Ensling, A. Sieber, A. Neels, H. Stoeckli-Evans, S. Decurtins, *Inorg. Chem.* 2005, **44**, 969-978; (b) D. P. Zhang, W. J. Si, P. Wang, X. Chen, J. Z. Jiang, *Inorg. Chem.* 2014, **53**, 3494-3502; (c) Y. Z. Zhang, O. Sato, *Inorg. Chem.* 2010, **49**, 1271-1273.

20 X. Y. Wang, A. V. Prosvirin, K. R. Dunbar, *Angew. Chem. Int. Ed.* 2010, **49**, 5081-5084.

21 G. Brauer, eds. *Handbook of Preparative Inorganic Chemistry*, vol. 2, Academic Press, New York, 2nd edn. 1965, p. 1473.

22 D. P. Zhang, H. L. Wang, Y. T. Chen, Z. H. Ni, L. J. Tian, J. Z. Jiang, *Inorg. Chem.* 2009, **48**, 5488-5496.

23 A. Dees, A. Zahl, R. Puchta, N. J. Hommes, F. W. Heinemann, I. Ivanovic-Burmazovic, *Inorg. Chem.* 2007, **46**, 2459-2470.

24 SAINT Version 7.68A, Bruker AXS, Inc.; Madison, WI 2009.

25 Sheldrick, G. M. SADABS, Version 2008/1, Bruker AXS, Inc.; Madison, WI 2008.

26 Sheldrick, G. M. SHELXTL, Version 6.14, Bruker AXS, Inc.; Madison, WI 2000-2003.

27 D. Casanova, P. Alemany, J. M. Bofill, S. Alvarez, *Chem. Eur. J.* 2003, **9**, 1281-1295.

28 N. F. Chilton, R. P. Anderson, L. D. Turner, A. Soncini, K. S. Murray, *J. Comput. Chem.* 2013, **34**, 1164-1175.

29 J. A. Mydosh, *Spin Glasses: An Experimental Introduction*, Taylor& Francis, London, 1993.

30 For examples of the “magnetic sponges”: (a) J. Larionova, S. A. Chavan, J. V. Yakhmi, A. G. Frøystein, J. Sletten, C. Sourissean, O. Kahn, *Inorg. Chem.* 1997, **36**, 6374-6381; (b) J. Milon, M. C. Daniel, A. Kaiba, P. Guionneau, S. Brandes, J. P. Sutter, *J. Am. Chem. Soc.* 2007, **129**, 13872-13878; (c) M. Fitta, R. Pełka, D. Pinkowicz, M. Bałanda, M. Czapla, M. Mihalik, D. Pinkowicz, B. Sieklucka, T. Wasiutyński, M. Zentkova, *Eur. J. Inorg. Chem.* 2012, 3830-3834.

Table of Content

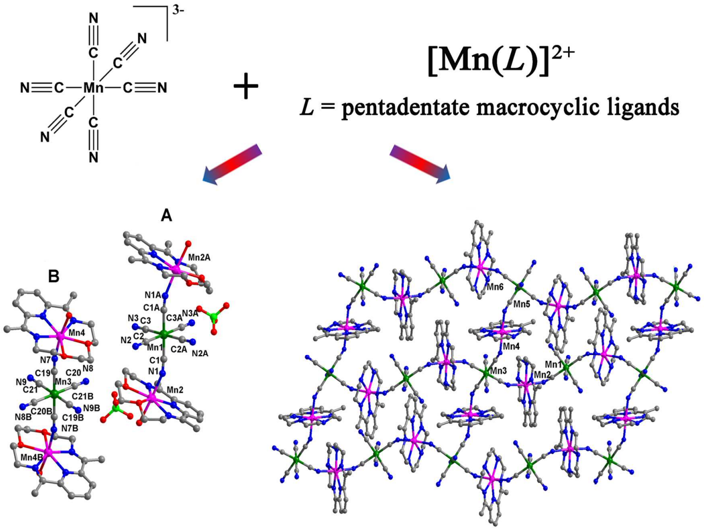

By tuning the reaction condition and using the macrocyclic ligands, three $[Mn(CN)_6]^{3-}$-based magnetic complexes were prepared and characterized.